



HAL
open science

AEgIS Experiment: Status & Outlook

P. Lansonneur, S. Aghion, C. Amsler, G. Bonomi, R.S. Brusa, M. Caccia, R. Caravita, F. Castelli, G. Cerchiari, D. Comparat, et al.

► **To cite this version:**

P. Lansonneur, S. Aghion, C. Amsler, G. Bonomi, R.S. Brusa, et al.. AEGIS Experiment: Status & Outlook. 52nd Rencontres de Moriond on Gravitation, Mar 2017, La Thuile, Italy. pp.87-92. hal-01815219

HAL Id: hal-01815219

<https://hal.science/hal-01815219>

Submitted on 8 Nov 2018

HAL is a multi-disciplinary open access archive for the deposit and dissemination of scientific research documents, whether they are published or not. The documents may come from teaching and research institutions in France or abroad, or from public or private research centers.

L'archive ouverte pluridisciplinaire **HAL**, est destinée au dépôt et à la diffusion de documents scientifiques de niveau recherche, publiés ou non, émanant des établissements d'enseignement et de recherche français ou étrangers, des laboratoires publics ou privés.

AEgIS Experiment: Status & Outlook

P. Lansonneur¹, S. Aghion^{2,3}, C. Amsler⁵, G. Bonomi^{6,7}, R. S. Brusa^{8,9}, M. Caccia^{3,10}, R. Caravita^{11,12}, F. Castelli^{3,14}, G. Cerchiari¹⁵, D. Comparat¹⁶, G. Consolati^{2,3}, A. Demetrio¹⁷, L. Di Noto^{11,12}, M. Doser¹³, C. Evans^{2,3}, R. Ferragut^{2,3}, J. Fesel¹³, A. Fontana⁷, S. Gerber¹³, M. Giammarchi³, A. Gligorova¹⁹, F. Guatieri^{8,9}, S. Haider¹³, A. Hinterberger¹³, H. Holmestad²¹, A. Kellerbauer¹⁵, O. Khalidova¹³, D. Krasnicky^{11,12}, V. Lagomarsino^{11,12}, P. Lebrun¹, C. Malbrunot^{13,5}, S. Mariazzi⁵, J. Marton⁵, V. Matveev^{22,23}, Z. Mazzotta^{3,14}, S. R. Müller¹⁷, G. Nebbia²⁴, P. Nedelec¹, M. Oberthaler¹⁷, N. Pacico¹⁹, D. Pagano^{6,7}, L. Penasa^{8,9}, V. Petracek²⁰, F. Prelz³, M. Prevedelli²⁵, L. Ravelli^{8,9}, B. Rienaecker¹³, J. Robert¹⁶, O. M. Rhøne²¹, A. Rotondi^{7,26}, M. Sacerdoti^{3,14}, H. Sandaker²¹, R. Santoro^{3,10}, M. Simon⁵, L. Smestad^{13,28}, F. Sorrentino^{11,12}, G. Testera¹², I. C. Tietje¹³, E. Widmann⁵, P. Yzombard¹⁶, C. Zimmer^{13,15,3}, J. Zmeska⁵, N. Zurlo^{7,29}.

¹Institute of Nuclear Physics, CNRS/IN2p3, University of Lyon 1, 69622 Villeurbanne, France

²Politecnico of Milano, Piazza Leonardo da Vinci 32, 20133 Milano, Italy

³INFN Milano, via Celoria 16, 20133, Milano, Italy

⁵Stefan Meyer Institute for Subatomic Physics, Austrian Academy of Sciences, Boltzmanngasse 3, 1090 Vienna, Austria

⁶Department of Mechanical and Industrial Engineering, University of Brescia, via Branze 38, 25123 Brescia, Italy

⁷INFN Pavia, via Bassi 6, 27100 Pavia, Italy

⁸Department of Physics, University of Trento, via Sommarive 14, 38123 Povo, Trento, Italy

⁹TIFPA/INFN Trento, via Sommarive 14, 38123 Povo, Trento, Italy

¹⁰Department of Science, University of Insubria, Via Valleggio 11, 22100 Como, Italy

¹¹Department of Physics, University of Genova, via Dodecaneso 33, 16146 Genova, Italy

¹²INFN Genova, via Dodecaneso 33, 16146 Genova, Italy

¹³Physics Department, CERN, 1211 Geneva 23, Switzerland

¹⁴Department of Physics, University of Milano, via Celoria 16, 20133 Milano, Italy

¹⁵Max Planck Institute for Nuclear Physics, Saupfercheckweg 1, 69117 Heidelberg, Germany

¹⁶Laboratoire Aimé Cotton, Université Paris-Sud, ENS Cachan, CNRS, Université Paris-Saclay, 91405 Orsay Cedex, France

¹⁷Kirchhoff-Institute for Physics, Heidelberg University, Im Neuenheimer Feld 227, 69120 Heidelberg, Germany

¹⁸Department of Physics, Heidelberg University, Im Neuenheimer Feld 226, 69120 Heidelberg, Germany

¹⁹Institute of Physics and Technology, University of Bergen, Allégaten 55, 5007 Bergen, Norway

²⁰Czech Technical University, Prague, Brehova 7, 11519 Prague 1, Czech Republic

²¹Department of Physics, University of Oslo, Sem Saelandsvei 24, 0371 Oslo, Norway

²²Institute for Nuclear Research of the Russian Academy of Science, Moscow 117312, Russia

²³Joint Institute for Nuclear Research, 141980 Dubna, Russia

²⁴INFN Padova, via Marzolo 8, 35131 Padova, Italy

²⁵University of Bologna, Viale Berti Pichat 6/2, 40126 Bologna, Italy

²⁶Department of Physics, University of Pavia, via Bassi 6, 27100 Pavia, Italy

²⁷Department of Physics “Ettore Pancini”, University of Napoli Federico II, Complesso Universitario di Monte S. Angelo, 80126, Napoli, Italy

²⁸The Research Council of Norway, P.O. Box 564, NO-1327 Lysaker, Norway

²⁹Department of Civil Engineering, University of Brescia, via Branze 43, 25123 Brescia, Italy

The AEGIS experiment ¹ (Antimatter Experiment: Gravity, Interferometry, Spectroscopy) is planned to perform the first measurement of the gravitational acceleration on antimatter by observing the free fall of antihydrogen atoms. By combining techniques based on recent developments in the production of positronium and its laser excitation to Rydberg states, such a study seems indeed to be feasible for neutral antimatter. We present here some of the experimental techniques involved in the experiment as well as the status of the detector test envisioned for the gravity measurement.

1 Scientific goal and challenges

The weak equivalence principle states that the motion of a particle is independent of its composition and internal structure when submitted to gravity. Although several attempts were made in the past to test this principle with antiprotons² or positrons³, they lead to large uncertainties mainly due to difficulties to control coulombian effects. For this reason, neutral antihydrogen atoms, benefiting from the extensive experimental developments achieved in the 1990's at CERN appear thus to be good candidates. The goal of the AEGIS experiment is to test the weak equivalence principle for neutral antihydrogen ($\bar{\text{H}}$ in the following). The challenging idea is to produce a beam of cold anti-atoms by charge-exchange reaction, involving antiprotons ($\bar{\text{p}}$), provided by the antiproton decelerator (AD) at CERN and positronium (Ps), a bound-state of electron and positron:



This reaction reveals several advantages. Indeed, the corresponding cross-section evolves as n^4 with n the principal quantum number of positronium, which represents ¹ $\sigma \sim 10^{-9} \text{ cm}^2$ for $n = 25$. Moreover, as the principal quantum number of the antihydrogen is linked with n , the final state distribution can be controlled by correctly tuning the laser excitation¹. But since the measurement of the gravitational acceleration will rely on the vertical deflection of the beam induced by gravity, the uncertainty on the velocity of the antihydrogen atoms represents one of the largest systematic error of the measurement. The whole experiment is hence performed in a cryogenic environment (liquid helium).

2 Positronium formation and excitation

In order to form a dense positronium cloud, positrons emitted by a radioactive ²²Na source, are ejected onto a nanoporous silica target. Among the two possible spin configurations (aligned or anti-aligned), the ortho-positronium, triplet state decaying into three gammas, has a particularly long lifetime of 142 ns.

One important achievement of AEGIS in 2016 is the creation of positronium inside the main apparatus. To detect its formation, the annihilation of the electron and the positron nearby the target was observed by the mean of plastic scintillators surrounding the AEGIS apparatus. The technique of Single Shot Positron Annihilation Lifetime Spectroscopy (SSPALS) enabled then to extract from the spectrum of the annihilation counts as a function of the time, the lifetime of positronium, in our case equal to $142.8 \pm 1 \text{ ns}$.

To increase the cross-section of the charge-exchange reaction, the positronium is excited by two lasers. A first ultra-violet laser ($\lambda = 205 \text{ nm}$) allows the transition from ground state to $n = 3$ while an infrared laser ($\lambda = 1064 \text{ nm}$) excite the antihydrogen to $n \sim 35$. The SSPALS spectrums of positronium with and without laser excitation, recorded outside from the main apparatus, are displayed in figure 1 (left). The plot on the right is obtained by subtracting the area below the two dark gray curves on the left as a function of the ultra-violet laser wavelength, tuned by adjusting the temperature of an optical parametric generator crystal. The spread of the curve, centered on the $n = 1$ to $n = 3$ transition wavelength, is directly linked to the

velocity distribution of the positronium cloud (Doppler broadening). A proper modeling allows one to extract from this curve the spread in velocity of the positronium atoms⁴, of the order of $\sigma_v = 10^5$ m/s.

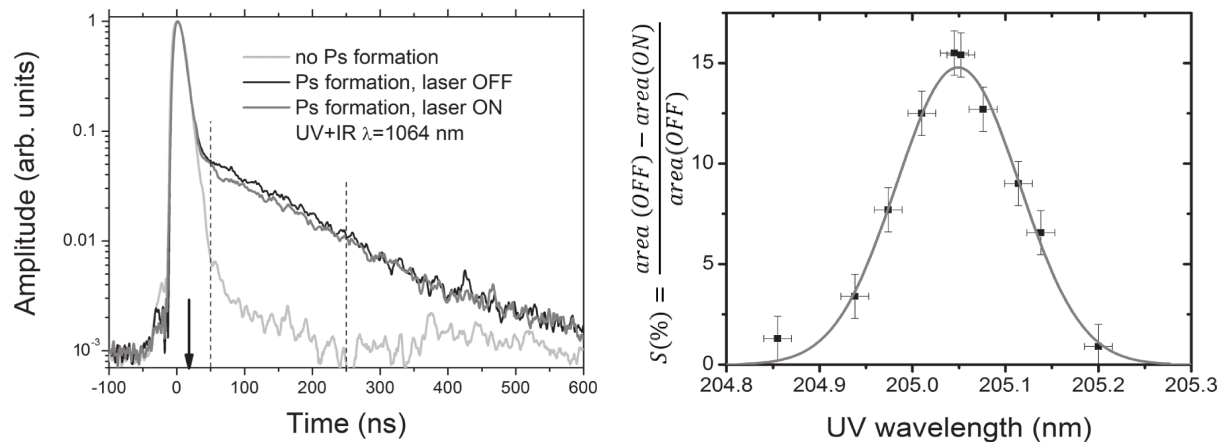


Figure 1 – (left) The SSPALS spectrum of positronium with and without laser excitation. As the positronium is excited to a state with longer lifetime, it contributes less to the beginning of the spectrum (the curve with laser ON is below the one with laser OFF). (right) The difference of the two curves in dark gray on the left as a function of the UV laser wavelength, corresponding to the $n = 1$ to $n = 3$ transition. The spread gives the velocity spread of the positronium cloud (Doppler broadening).

3 Antiprotons manipulations

The confinement of the antiprotons in the AEGIS setup is ensured by a set of Penning-Malmberg traps. In such traps, an axial magnetic field ensures the confinement of the particles radially while the longitudinal motion is restricted by applying a potential well on a set of ring-shaped electrodes. A view of the AEGIS trap system along with some of the main diagnostics is shown in figure 2.

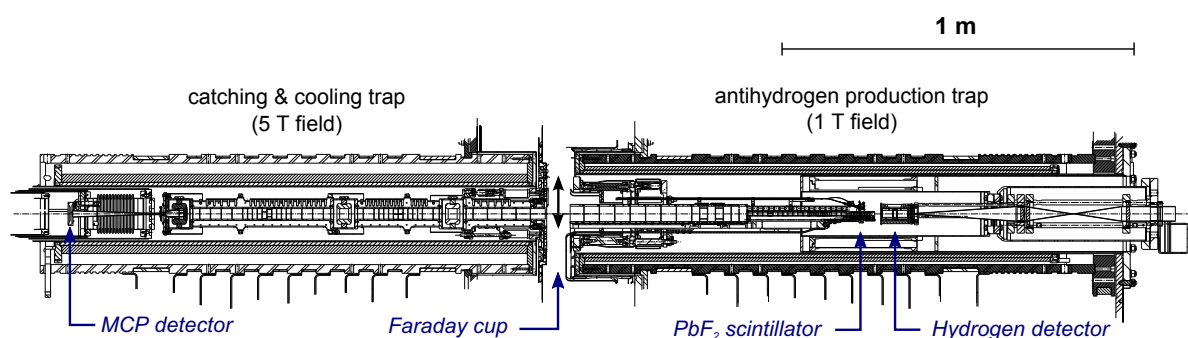


Figure 2 – Schematic view of the AEGIS traps as well as some of the detectors (blue). The cryogenic tanks surrounding the superconducting magnets are not displayed. The antiprotons exiting the AD and passing through a thin degrader from the left side are caught and cooled by electron sympathetic cooling within the trap placed in a 5 T axial field (left). A microchannel plate (MCP) as well as a segmented Faraday cup are the main diagnostics for this region of the apparatus. Once cold, the antiprotons are sent toward the 1 T trap, divided into two parts: the off-axis trap, where the positrons are transmitted toward the positronium converter, and the on-axis trap where the antihydrogen production occurs. A scintillator placed nearby the positronium converter allows one to monitor the formation of positronium. The antiproton manipulations in the 1 T region are controlled by the mean of the hydrogen detector, consisting of three ionizing electrodes stacked to a MCP.

Several steps are needed to prepare and transfer the antiprotons to the production region. The procedure adopted in AEGIS is the following:

1. Approximately 10^8 electrons are loaded in the 5 T trap. Within a few milliseconds, they cool down to the cryogenic temperature by radiative cooling;
2. A bunch of $3 \cdot 10^7$ antiprotons at 5.3 MeV are delivered every 110 seconds by the antiproton decelerator. After passing through a thin degrader to reduce their energy, the fraction with an energy below a few keV is caught in the 5 T trap;
3. By coulombian collisions, the antiprotons transfer their energy to electrons which in turns radiate within a few ms (sympathetic cooling). The time needed for the antiproton temperature to stabilize is typically of the order of one minute;
4. The antiprotons are compressed by applying an oscillating potential on a an electrode segmented azimuthally (“Rotating Wall” technique) and are finally sent toward the trap where the production is planned to occur, located in the 1 T region. This step reaches now 90 % of efficiency such that around $3 \cdot 10^5$ antiprotons are stored into the production trap for each shot of the AD.

4 Gravity measurement

Once the antihydrogen produced, the value of the gravitational acceleration for antimatter is proposed to be measured using a moiré deflectometer. It consist of three transmission gratings having a pitch d and separated by a distance L . As shown in figure 3, under the effect of gravitation, massive particles experience an acceleration a in the vertical direction leading to a parabolic trajectory while undeflected particles such as photons conserve straight trajectories throughout the whole apparatus⁷. The shift Δy between the two impacts at the level of the third grating is then given by:

$$\Delta y = a\tau^2 \quad (2)$$

where $\tau = L/v_z$ is the time of flight between two gratings. For an apparatus length of 1 meter and assuming a Maxwellian distribution of the particles velocity around a few Kelvins, it leads to a typical spatial shift of $50 \mu\text{m}$ for $a = 9.81 \text{ m.s}^{-2}$. Such a small shift can however be problematic to measure with standard particle detectors. Adding a third grating with the same pitch d but tilted by a small angle allows one to take advantage of the moiré effect to reveal macroscopic fringes orthogonal to the slits orientation. More details can be found in reference⁶.

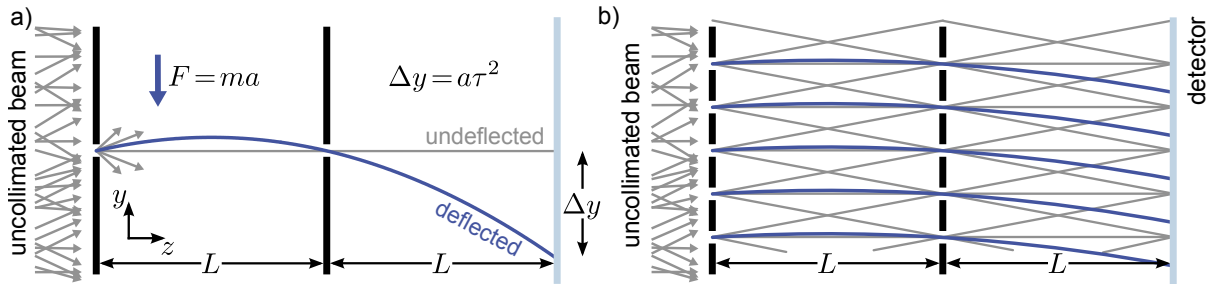


Figure 3 – a) Two slits separated by a distance L restrict the path of a beam to a specific trajectory. b) Replacing the slits by two gratings increases the flux of particles reaching the detector. A third grating (not shown here) located at the level of the detector allows one to take advantage of the moiré effect to reveal macroscopic fringes.

Several imaging detectors are envisioned for the gravity measurement. Two candidates are currently being tested on a secondary beamline: the nuclear emulsions and a silicon detector. The nuclear emulsions consist of plates of plastic covered with AgBr(I) crystals distributed homogeneously in a gelatin substrate. When excited by a charged particle, the annihilation products, such as pions, imprint on the emulsion plate a latent image. But in spite of their impressive imaging capabilities (able to reconstruct the antiproton annihilation vertices with a precision of 2 microns), the emulsions films require to open regularly the vacuum chamber and need a large amount of time to be processed. For these reasons, the choice has been oriented toward silicon detectors whose time capabilities of nanoseconds represent no issue. Among the detectors being tested, the Timepix⁸, initially developed for medical imaging applications, is able to determine with 25 microns resolution the position of an antiproton annihilation with 56 % tagging efficiency⁹.

5 Conclusion

The results of last antiproton runs have been numerous with the achievement of positronium formation in the production region, its excitation to $n = 3$ outside from the main apparatus, the transfer of around 10^5 antiprotons per shot in the production trap and the tests of possible detectors envisioned for gravity measurement. Before the long shutdown of the LHC planned from 2019 to 2021, the plan is now to produce antihydrogen in the AEGIS setup and to perform a first gravity measurement.

References

1. G. Y. Drobychev et al., Proposal for the AEGIS experiment at the CERN antiproton decelerator (Antimatter Experiment: Gravity, Interferometry, Spectroscopy), 2007.
2. N. Beverini et al., PS200 proposal Preprint, Los Alamos National Laboratory report LAUR-86-260, 1986.
3. F. Witteborn and W. Fairbank, Phys Rev Lett 19, 1049, 1967.
4. S. Aghion et al., Laser excitation of the $n = 3$ level of positronium for Antihydrogen production, Physical Review A 94 (2016).
5. S. Maury, The antiproton decelerator: AD, Hyperfine Interactions, 109(1), 43-52, 1997.
6. M. K. Oberthaler, S. Bernet, E. M. Rasel, J. Schmiedmayer, & A. Zeilinger, Inertial sensing with classical atomic beams, Physical Review A, vol. 54, num 4, 1996.
7. P. Bräunig, Atom Optical Tools for Antimatter Experiments, Heidelberg University PhD thesis (2015).
8. T. Poikela et al., Timepix3: a 65K channel hybrid pixel readout chip with simultaneous ToA/ToT and sparse readout, Journal of instrumentation, 9(05), C05013, 2014.
9. H. Holmestadt. Analysis of the 2015 data. GRACE/ATLIX internal note, Oct. 2016.

